

## TURBULENCE-INDUCED MAGNETIC FIELDS AND STRUCTURE OF COSMIC RAY MODIFIED SHOCKS

A. BERESNYAK<sup>1</sup>, T. W. JONES<sup>2</sup>, A. LAZARIAN<sup>1</sup>  
 Dept. of Astronomy, Univ. of Wisconsin, Madison, WI 53706  
*Draft version July 31, 2021*

### ABSTRACT

We propose a model for Diffusive Shock Acceleration (DSA) in which stochastic magnetic fields in the shock precursor are generated through purely fluid mechanisms of a so-called small-scale dynamo. This contrasts with previous DSA models that considered magnetic fields amplified through cosmic ray streaming instabilities; i.e., either by way of individual particles resonant scattering in the magnetic fields, or by macroscopic electric currents associated with large-scale cosmic ray streaming. Instead, in our picture, the solenoidal velocity perturbations that are required for the dynamo to work are produced through the interactions of the pressure gradient of the cosmic ray precursor and density perturbations in the inflowing fluid. Our estimates show that this mechanism provides fast growth of magnetic field and is very generic. We argue that for supernovae shocks the mechanism is capable of generating upstream magnetic fields that are sufficiently strong for accelerating cosmic rays up to around  $10^{16}$  eV. No action of any other mechanism is necessary.

*Subject headings:* turbulence, MHD, shock waves, cosmic rays, scattering, acceleration of particles

### 1. INTRODUCTION

Cosmic rays (CRs), relativistic charged particles with energies  $10^8 - 10^{22}$  eV, constitute an essential part of astrophysical systems (see Schlickeiser 2003). In galaxies they often provide pressure and energy densities comparable to those of magnetic fields and thermal gas. In very dense regions, such as the cores of molecular clouds or accretion disks they are the only source of ionization that that must be present to allow interaction of magnetic field and the fluid (see McKee & Ostriker 2007). The origin of CRs has been a subject of debate from the beginning of research in the field (Ginzburg & Syrovatsky 1964). By now, it is accepted, however, that galactic CRs at least up to the “knee” in the spectrum just above  $10^{15}$  eV are most likely generated primarily by strong supernova shocks.

The modern study of CR acceleration in shocks involving so-called diffusive shock acceleration (DSA) began with Krymsky (1977) and Bell (1978) test particle models. They noted that when particles whose mean free paths exceed the thickness of a viscous shock are scattered upstream and downstream of the shock on ideal scatterers moving with the bulk fluid, they gain energy each time they return across the shock front. The resulting steady-state CR distribution is a power-law in momentum, ( $f \propto p^{-q}$ ) with a slope  $q = 4M^2/(M^2 - 1)$ , where  $M$  is the shock flow Mach number. This asymptotes to  $q = 4$  for strong shocks. It soon became apparent, if there is efficient injection of fresh CRs at the shock, that CRs can extract significant energy from the shocked flow. Since the CRs diffuse ahead of the shock, this naturally leads to a pressure gradient upstream of the shock transition that smoothly decelerates and compresses flow into the shock, forming a shock precursor. In strongly modified shocks, the total velocity jump through the precursor can exceed that for a classical adiabatic

fluid shock. Since CRs with higher energies usually have longer mean free paths, they travel further into the precursor than lower energy CRs. Consequently, they “see” a stronger shock transition, and are accelerated more efficiently. This leads to an upward-concave spectrum reaching a somewhat shallower slope than the test particle spectrum at large energies (Malkov & Drury 2001 and ref. therein).

On the other hand, the scattering events encountered by the CRs are not ideal, but depend on some complex physics determined by details of the local electromagnetic field, which is, in turn, modified by the CRs. In a diffusive propagation approximation one must pay close attention to this local physics to determine the spatial diffusion coefficient,  $D_{xx}$ , and the momentum diffusion coefficient,  $D_{pp}$ , that go into the diffusion-convection equation for the quasi-isotropic CR distribution function  $f$ :

$$\frac{\partial f}{\partial t} + u \frac{\partial f}{\partial x} = \frac{\partial}{\partial x} \left( D_{xx} \frac{\partial f}{\partial x} \right) + \frac{p}{3} \frac{\partial u}{\partial x} \frac{\partial f}{\partial p} + \frac{1}{p^2} \frac{\partial}{\partial p} \left( p^2 D_{pp} \frac{\partial f}{\partial p} \right), \quad (1)$$

(e.g., Skilling 1975), with some source term added for injection and assuming that  $f(x, p)$  depends only on one spatial coordinate  $x$  and the magnitude of CR momentum,  $p$ . This equation uses the so-called “local” system of reference, where the particle momentum is measured with respect to the rest frame of the fluid. Similarly, magnetic field perturbations that are the driver of particle scattering should also be defined locally over the scales that are sampled by a particle gyrating in the magnetic field<sup>3</sup> (see, e.g., Yan & Lazarian 2004).

<sup>3</sup> Fortunately, the modern theory of strong MHD turbulence, which uses a notion of “critical balance” (Goldreich & Sridhar 1995), is formulated in the terms of local, rather than global field (see Cho & Vishniac 2000, Maron & Goldreich 2001, Beresnyak &

<sup>1</sup> Dept. of Astronomy, Univ. of Wisconsin, Madison, WI 53706

<sup>2</sup> Dept. of Astronomy, Univ. of Minnesota, Minneapolis, MN 55455

As the fluid and the high-energy particles couple through the electromagnetic field, the problem reduces in practice to the study of the generation of magnetic fields, their spatial structure and the scattering of particles in those fields. This problem, formulated in the most general case (e.g. with the fully three-dimensional Vlasov's equation) is very hard to treat. In part this is due to the nonlinear nature of the coupling between particles and fields. Following the original test particle model a number of approaches to include more complete physics have been adopted in the literature. One of the most popular approaches to capture the feedback of CRs on the electromagnetic fields has been to apply the streaming instability mechanism, where particles, escaping upstream along the magnetic field, confine themselves by amplification of resonant waves (Lagage & Cesarsky 1983). This approach assumes the existence of the background magnetic field, which is usually taken for simplicity to be directed perpendicular to the shock; that is, along the shock normal. This field was traditionally assumed to be of the order of the background ISM magnetic field,  $B_0 \sim 5\mu G$ .

However, it is easy to show that upstream magnetic fields of around  $5\mu G$  are too weak to provide an efficient acceleration of the cosmic rays with energies as high as  $10^{15}$  GeV, as required for supernova shocks to produce CRs to the knee. PeV cosmic rays have long mean free paths in such a field and have a high probability of escaping the shock, so they are not subject to further acceleration. This poses a serious problem for the shock acceleration of galactic CRs.

To overcome the problem one can argue that the magnetic field in the preshock region can be much stronger than its interstellar value and that the free energy available for the shock is sufficient to generate much larger fields (Volk, Drury & McKenzie, 1984). The magnetic field generation, if pursued through streaming instability, leads naturally to a highly nonlinear stage of the streaming instability where  $\delta B \gg B_0$ . The original classical treatment of the instability is not applicable in that limit. What happens in the non-linear regime has been a subject of much discussion in recent years (e.g., Lucek & Bell 2000, Diamond & Malkov 2007, Blasi & Amato 2008, Zirakashvili et al 2008, Riquelme & Spitkovsky 2009). The current driven instability proposed by Bell (2004) has moved recently to the center of this scientific debate. The driving electric current of that instability comes from drift (streaming) of the escaping CRs. The *compensating* return current of the background plasma leads to a transverse force on the background plasma that can amplify transverse perturbations in the magnetic field. Numerical simulations suggest that the initial field strength can grow substantially, leading in the nonlinear form to disordered fields with coherence lengths that depend on field strength (Bell 2004, Zirakashvili et al 2008, Riquelme & Spitkovsky 2009).

CR streaming instability in the presence of a relatively organized magnetic field is an attractive starting point in understanding how CRs may amplify magnetic fields. We argue, on the other hand, that the classic treatment

of streaming instability can not deal with  $\delta B \gg B_0$  case, i.e., can not generate large fields directly. This is because a large perturbed field violates the key assumptions of particle dynamics made in establishing the instability. Various attempts have been made to “renormalize” the magnetic field so that the perturbation  $\delta B$  becomes a new effective  $B_0$ . For instance, Diamond and Malkov (2007) considered diffusion of magnetic energy from resonant gyro-scales to larger scales due to compressibility effects. Among their assumptions were weak coupling and advection-diffusion equations for wave number densities<sup>4</sup>. Like most treatments of this problem, their equations were also one-dimensional in space, which required relatively simple structure of the cosmic ray density with respect to magnetic field direction. The case of a highly tangled three-dimensional magnetic field with  $\delta B \gg B_0$ , which is the case we explore here, can not be treated in such way.

Indeed, in following a magnetic field line one will typically see regions with alternating direction of the CR density gradient. Therefore, streaming CRs will produce both forward and backward going waves. This is unlike the classic picture where mostly forward-going waves are produced. In a turbulent field those regions of the alternating CR gradient will be non-trivially determined by the topology of the field and the details of CR diffusion (see Appendix A).

Is it possible to generalize the streaming instability approach to be applicable in a tangled magnetic field by arguing that each particle scattering creates a magnetic field perturbation on its own gyro-scale? The difficulty with this is that in the tangled  $\delta B \gg B_0$  field such small incoherent perturbations are going to average out, leaving the basic, residual effect that the CRs apply pressure to the fluid. Can substantial magnetic fields be efficiently generated in this generic case? This is the subject of the present paper.

In what follows, we argue that there is an alternative process that can provide fast magnetic field generation. It provides sufficiently strong magnetic field without appealing to either classical streaming instabilities or their modifications. The CR pressure gradient is the dynamical agent that forms the shock precursor and also drives field amplification<sup>5</sup>.

We discuss below the generation of a strong magnetic field as the precursor interacts with the interstellar medium. We assume that the CR pressure is a smooth function applied to the fluid, while the magnetic field is generated by purely fluid nonlinear mechanisms. The magnetic field, in turn, plays the role of CR scatterer and accelerator. The fluid is stirred within the precursor on large, precursor-sized, scales by the combination of fluid

<sup>4</sup> The assumption of weak coupling is broken in the case of strongly interacting waves, which necessarily appear in MHD turbulence (Goldreich & Sridhar 1995), while the Fokker-Planck assumption is often broken even in the case of weak coupling, e.g., when the interaction is mediated by wavevectors of comparable magnitude (Galtier et al 2000, Chandran 2005).

<sup>5</sup> This physics clearly depends on prior development of a strong CR precursor to the shock. That requires waiting only until the shock is able to accelerate CRs to relativistic energies (e.g., Kang et al. 2009). Even microGauss level fields, without strong amplification, can do that quickly. For instance standard diffusive shock acceleration using Bohm diffusion with a 1  $\mu G$  field in a 10,000 km/s shock produces GeV CRs on a timescale of about a year.

Lazarian 2009a,b). How the turbulence may be modified in the presence of cosmic rays is still of an open question, however (see, e.g., Lazarian & Berezhnaya 2006).

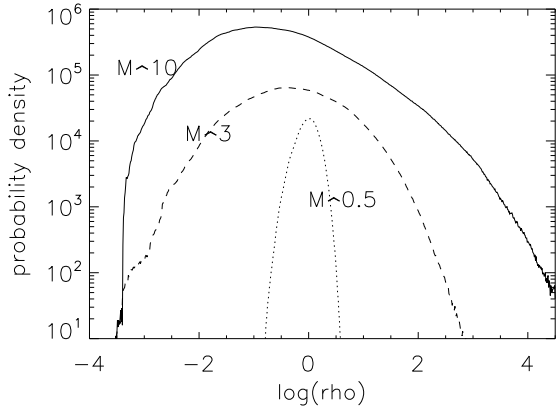


FIG. 1.— PDF of density of the inflow fluid is approximately log-normal due to the ambient turbulence in the ISM. Pictured is the PDF of density from simulations with different sonic Mach numbers (Beresnyak, Lazarian & Cho, 2005).

density inhomogeneities and CR pressure. Although we consider the CR pressure applied to the inflowing fluid homogeneous in the direction along the shock, the acceleration of the fluid element is highly inhomogeneous due to the density inhomogeneity of the fluid. This drives precursor turbulence. The magnetic energy is generated on intermediate scales through a small-scale dynamo. While the cosmic ray pressure gradient is smooth, the generated magnetic field is tangled and effectively suppresses the streaming instabilities, at least in their classical formulation. In assuming a smooth CR pressure distribution, we are effectively averaging the CR action over small scales. We leave the problem of the fluctuations of CR and magnetic pressure on gyroscale to future study<sup>6</sup>.

## 2. PRECURSOR-GENERATED VELOCITY FIELD

Although in a classic hydrodynamic shock no information can travel upstream and create perturbations, the upstream diffusion of CRs leading to precursor formation makes this possible, since CRs are much faster than the inflow. Because CRs couple only diffusively to the fluid, their distribution will generally be smoother and only slowly reactive to local changes in the fluid. This creates a number of new possibilities, such as the Drury acoustic instability (Drury 1984; Dorfi & Drury 1985; Kang et al. 1992), which is the enhancement of compressible perturbations by the CR pressure gradient. Such instabilities, however, will only operate on perturbations during the limited time that a fluid element crosses the precursor. This crossing time  $\tau_c$  will be determined by the flow profile as

$$\tau_c = \int_{x_0}^0 \frac{dx}{u(x)}. \quad (2)$$

On the other hand, generically, a fluid element passing through the precursor has inhomogeneities of its own. Some level of density inhomogeneity is always present in astrophysical plasmas, including the ISM (Armstrong et

<sup>6</sup> In strongly CR modified shocks the acceleration of high energy particles mostly takes place within the precursor. Furthermore, in those shocks the CR pressure is predominantly in high-energy particles. As we will see in §3 those particles do not have a gyroscale with the conventional meaning.

al. 1995) and stellar winds, media that typically transmit SNR shocks. These inhomogeneities, covering an extended range of scales, are usually associated with MHD turbulence<sup>7</sup> (see, e.g., Elmegreen & Scalo 2004, Lazarian & Opher 2009). Also there are so-called Small Ionized and Neutral (SIN) structures, which exhibit fluctuations at the scale from 100 to 1000 AU that are order of magnitude larger in amplitude than those expected from the simplistic extension of the turbulent cascade to small scales<sup>8</sup> (Heiles, 1997). The stellar winds, acting as media through which many young supernova shocks propagate, are also inhomogeneous and turbulent.

Another generic property of the ISM and winds is cooling (radiative, collisional, etc). Cooling keeps temperatures fairly low, which makes ISM fluids pliable to compression. The typical Mach numbers in the warm ISM are observed to be between 1 and 10. Such strongly compressive flows are characterized by significant nonlinear perturbations of density<sup>9</sup>. The hot ISM is usually subsonic with respect to ambient turbulence, which suggests smaller magnitude of the perturbations of density.

As inhomogeneous fluid flows into the precursor with speed  $u_0$  it is gradually decelerated by the CR pressure gradient until it reaches the speed  $u_1$  at the dissipative shock front (Fig. 2). This deceleration could create perturbations of velocity of the order  $u_0 - u_1$ , a difference between ballistic velocity of the high-density region and full deceleration of the low density regions. The resulting velocity field could not be purely divergent, but should be partially solenoidal due to the coupling between compressible and solenoidal motions on the outer scale of supersonic turbulence<sup>10</sup>. Simulations of strongly compressible turbulence normally show a 2:1 ratio of solenoidal to compressive motions, corresponding to 2:1 degrees of freedom in velocity. However, this ratio was observed in simulations of statistically isotropic stationary turbulence, while in our problem we have a preferred direction, perpendicular to the shock front and a limited time for the turbulence to develop. Taking into account our lack of knowledge of the precursor highly compressible turbulence we parameterize the amount of solenoidal motions with a parameter  $A_s$  such as the RMS of the solenoidal part of the velocity  $u_s$  be defines as

$$u_s = A_s(u_0 - u_1), \quad (3)$$

where  $A_s$  could be of the order of unity or smaller. We designate the characteristic scale of solenoidal perturbations as  $L$ , Normally, the supersonic ISM exhibits large density perturbations on a wide range of scales. This is due to the fact that those are created mostly by ISM tur-

<sup>7</sup> Turbulence arises due to the fact that microscopic dissipation coefficients such as viscosity and magnetic diffusivity are small and the Reynolds numbers are huge, which makes laminar flows in space a practical impossibility.

<sup>8</sup> The origins of these inhomogeneities are still debated.

<sup>9</sup> A log-normal distribution of density is predicted and observed in simulations, see, e.g., Beresnyak, Lazarian & Cho (2005), for the supersonic isothermal magnetized turbulence, see Fig. 1, while the subsonic case usually has a normal distribution (which is a special case of log-normal)

<sup>10</sup> An easy way to visualize the effect of generation of the solenoidal motions is to consider the density inhomogeneities as random obstacles that interact with the flow. It is natural, that the flow get a solenoidal component as a result of such an interaction.

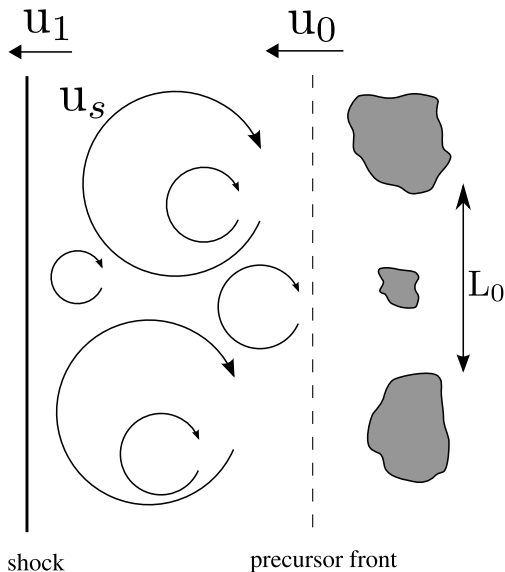


FIG. 2.— Solenoidal motions, excited by CR precursor (the real picture is three-dimensional). In the frame of the shock the pre-existing perturbations enter the precursor creating both compressive and solenoidal velocity perturbations (the last being depicted).

bulent slow sub-shocks. Although each secondary slow sub-shock typically has a moderate Mach number ( $\sim 2$ ), a random action of many sub-shocks creates regions of high over-density or under-density that can in rare instances exceed factors at least  $10^4$  (see, e.g., Beresnyak, Lazarian & Cho 2005). More generally, the density perturbation from individual sub-shocks is of order unity. The characteristic scale here is the distance between slow sub-shocks, which is smaller than the turbulence outer scale, and could be of order of parsecs. From a practical point of view, we will take  $L$  from one of the typical scales of the problem, either the above distance between sub-shocks or the thickness of the precursor, or dynamical length  $u_s \tau_c$ , whichever is smaller<sup>11</sup>.

In this paper we only consider turbulence hydrodynamically amplified within the precursor. We do not consider post-shock turbulence, which is a fairly well-known and better explored phenomenon that exists even in pure hydrodynamics without a CR precursor (see, e.g., Giacalone & Jokipii, 2007). For the purposes of this paper a rather simplistic description of the post-shock magnetic fields is sufficient. It is well known that strong fast shocks amplify magnetic field parallel to the shock front by, approximately, the shock compression ratio  $u_1/u_2$  (where  $u_2$  is the post-shock velocity). Using that approximation we will conservatively assume that the post-shock region has the same magnetic field structure as the precursor, but with magnetic field strength larger by a factor of  $\sqrt{2/3}u_1/u_2$ .

### 3. THE SMALL-SCALE DYNAMO

<sup>11</sup> Here we assumed that CR precursor is already mature, i.e., the CR pressure is a considerable fraction of shock pressure and the significant part of CR energy is in high-energy particles, which makes precursor relatively thick. We leave the bootstrap mechanism of the precursor to the future study.

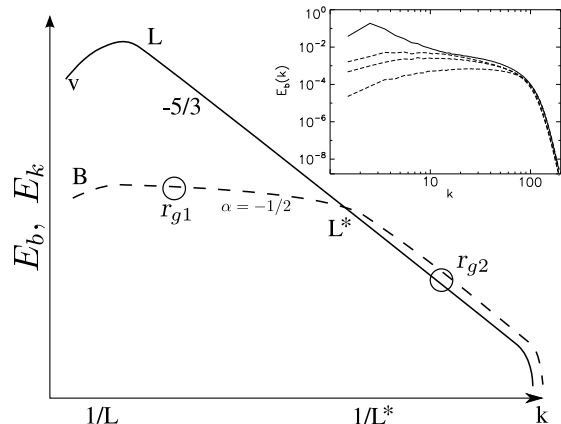


FIG. 3.— Magnetic field spectrum (dashed), generated by a small-scale dynamo induced by solenoidal velocity motions (solid).  $L^*$  is an equipartition scale of magnetic and kinetic motions, it plays a central role in particle scattering. Upper panel: magnetic and velocity fields from simulations (Cho et al 2009) with different dashed lines corresponding to magnetic spectra at different times.

Three-dimensional solenoidal flows can amplify magnetic fields through the stretch-fold mechanism. This refers not only to turbulent flows, which have motions on all scales, but even to large scale three-dimensional laminar flows (e.g., Zeldovich et al, 1984). In other words, amplification of magnetic fluctuations on small scales is a very generic feature of highly-conducting fluids. We will consider a so-called generic small-scale dynamo (turbulent) in which magnetic fields are amplified by initially weakly magnetized hydrodynamic turbulence with an energy-containing (outer) scale of  $L$ . “Small-scale” means that the scales of magnetic fields we are interested in are smaller than  $L$ . The problem of the so-called mean-field dynamo, when *large-scale* magnetic fields are generated by small-scale motions is not considered here, because the mean-field dynamo is fairly slow (see Vishniac & Cho 2001), while inside the shock precursor the time for the amplification is rather limited, since all perturbations are quickly advected to the dissipative shock. The small-scale dynamo has three principal stages – a kinematic stage, when magnetic energy grows exponentially, a linear stage and a saturation stage (see Cho et al, 2009).

The kinematic stage of the dynamo has been studied extensively by analytic (Kazantsev 1968, Kulsrud & Anderson 1992) and numerical tools. The rising spectrum with magnetic energy  $E_B(k) \sim k^{3/2}$  down to magnetic dissipation scales was predicted and later observed in numerical simulations. For astrophysical applications the kinematic dynamo is irrelevant, since its characteristic saturation timescale is of the order of the smallest eddies, which is a tiny number compared to outer timescales. For our purposes we can always assume that the kinematic dynamo is saturated and the dynamo is in the linear stage.

In the linear stage magnetic energy grows linearly with time as

$$\frac{1}{8\pi} \frac{dB^2}{dt} = A_d \epsilon, \quad (4)$$

where  $\epsilon$  is the energy transfer rate of the turbulence, which can be estimated as  $\epsilon = \rho u_s^3/L$ , and  $A_d$  can be

called an *efficiency of the small-scale dynamo*. A typical spectrum of the velocity and the magnetic field in the linear stage is presented on Fig. 3. At each particular time when the dynamo operates, the magnetic field reaches equipartition with the turbulent velocity field on some scale  $L^*$ . This scale grows with time. On scales smaller than  $L^*$  magnetic and velocity perturbations form an MHD turbulent cascade with a fairly steep spectrum. On scales larger than  $L^*$ , the magnetic field has a fairly shallow spectrum and velocity has a Kolmogorov spectrum.

The law of linear growth can be understood as follows. The main cascade of energy is down-scale, but it is converted from a purely velocity cascade to an MHD cascade at a scale  $L^*$ . One can imagine that part of this energy cascades up (an inverse cascade) in the form of magnetic energy. Let us call this fraction  $A_d$ . In principle,  $A_d$  can depend on scale, i.e.,  $A_d(L^*)$ . However, by an argument similar to Kolmogorov's, if the inverse cascade mechanism is purely nonlinear, then, in the middle of the inertial interval there is no designated scale and, therefore, there is no dimensionless combination involving  $L^*$ . Therefore, the function  $A_d(L^*)$  has to be constant<sup>12</sup>. This gives a linear growth of energy. The linear growth can also be obtained if we assume that it takes *several* turnover times to reach equipartition on each successive step to larger and larger  $L^*$ <sup>13</sup>. A linear growth rate has been measured in Cho et al. (2009) as being close to  $A_d \approx 0.06$  which is the quantity we will use in this paper.

The shallow part of the magnetic spectrum between  $L$  and  $L^*$  normally has a slope  $\alpha$  between 0 and  $-1$ , as observed in simulations. We will need these constraints later, when we describe a model of particle scattering. We particularly favor a model with  $\alpha = -1/2$ . This model assumes that while magnetic fields on a scale  $L^*$  are generated by random eddies at the same scale  $L^*$  and contain most of the magnetic field energy, the larger scale fields come from equipartition of magnetic tension on scale  $l > L^*$ . This can be estimated as  $\delta B^2(l)/l$ , while the averaged magnetic tension comes from a number  $N = (l/L^*)^3$  of independent random eddies on scale  $L^*$ . This will give scalings  $\delta B(l) \sim l^{-1/4}$  and

$$E_B(k)k = \delta B^2(k) \sim k^{1/2}. \quad (5)$$

When  $L^*$  approaches  $L$ , the small-scale dynamo enters the saturation stage in which the magnetic field grows more slowly than in the previous linear stage. The saturation value of magnetic energy depends slightly on the level of the mean magnetic field (Cho et al. 2009). In our case the *mean* magnetic field can be considered negligible, as the typical Alfvén velocity of warm ISM ( $\sim 12$  km/s) is much smaller than the shock speed and associated turbulent speeds (see § 2). For the purpose of this paper, however, we won't need a saturation stage, since we have limited time available for amplification,  $\tau_c$  (see § 2), which

<sup>12</sup> This assumes locality of the small-scale dynamo. It is indirectly confirmed by the linear growth observed in simulations.

<sup>13</sup> Schekochihin & Cowley 2007 proposed a model assuming that equipartition is reached at approximately one turnover time, which gives a linear growth of magnetic energy. This would correspond to our model with  $A_d \sim 1$ .

is normally not enough to reach the saturation stage<sup>14</sup>.

From the linear stage growth we derive quantities  $\delta B^* = \delta B(L^*, x_1)$  and  $L^*(x_1)$  that we will need in the next section:

$$\delta B^2(L^*, x_1) = 8\pi A_d \epsilon \tau(x_1); \quad (6)$$

$$\frac{\delta B^*}{\sqrt{4\pi\rho}} = u_s \left( \frac{L^*(x_1)}{L} \right)^{1/3}; \quad (7)$$

and

$$\tau(x_1) = \int_{x_1}^{x_0} \frac{dx}{u(x)}; \quad (8)$$

$$L^*(x_1) = (2A_d u_s \tau(x_1))^{3/2} L^{-1/2}. \quad (9)$$

#### 4. PARTICLE SCATTERING AND SECOND-ORDER ACCELERATION

In this section we derive  $D_{xx}$  and  $D_{pp}$  of the fast particles in the tangled magnetic fields created by the small-scale dynamo. It should be noted that particle dynamics is considered in the rest frame of the fluid (see also § 1).

As it turns out, there are three different regimes of particle scattering, depending on the particle energy,  $E$ , (see Fig. 4). The magnetic spectrum, described in Fig. 3, corresponds to the characteristic magnetic field on a particular scale  $\delta B(l) \sim \sqrt{E(k)k}$ , which increases<sup>15</sup> with decreasing scale as  $l^{-\alpha/2-1/2} = l^{-1/4}$  for  $\alpha = -1/2$  from  $L$  until  $L^*$  and decreases with scale as  $l^{1/3}$  for  $l$  smaller than  $L^*$ .

If the particle energy is sufficiently low, the particle will, to the first approximation, gyrate around a mean field. Otherwise, its trajectory will be stochastic. In particular, if  $E \ll e\delta B(L^*)L^*$ , the particle will be gyrating along the mean field of  $\delta B^* = \delta B(L^*)$  with Larmor radius of  $r_{g2} = E/e\delta B^*$ . We will refer to these particles as low-energy and designate low energies as region (1) in Fig. 4. For low energy particles the scattering frequencies and acceleration will be determined by a turbulence-based formulae with a turbulence outer scale of  $L^*$  (the scale with largest magnetic field). We will consider this case in detail in § 4.2.

##### 4.1. High energy particle scattering

If the energy of the particle is higher than  $e\delta B(L^*)L^*$ , there is no gyration and the particle's trajectory is fairly stochastic. This is due to the fact that for this particle, the vector magnetic field will be partially averaged out on larger scales (so that  $\delta B_l \sim l^{-1/4}$ ). Let us assume that such a particle experiences a Bohm scattering and has a *mean free path* of

$$\begin{aligned} r_{g1} &= (E/e\delta B^*)^{\frac{2}{1-\alpha}} (L^*)^{-\frac{1+\alpha}{\alpha}} \\ &= (E/e\delta B^*)^{4/3} (L^*)^{-1/3} > L^*. \end{aligned} \quad (10)$$

Indeed, (a) – on such a scale, a particle will be deflected by an angle of the order of unity; (b) – the deflection

<sup>14</sup> Indeed,  $L/u_s < \tau_c$  and saturation requires many  $L/u_s$ , since  $A_d \ll 1$ .

<sup>15</sup> Provided that spectrum is sufficiently shallow,  $\alpha > -1$

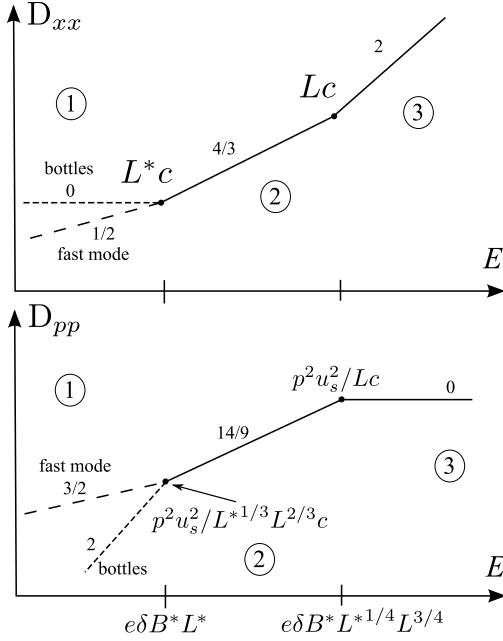


FIG. 4.— Scattering coefficients as they depend on energy. The scattering has three principal regimes: (1), low-energy scattering, which depends on the properties of small-scale MHD turbulence (two cases where fast modes are present (dashed) and absent (dotted) are shown); (2), strong scattering, where particles are scattered efficiently by the strong magnetic fields generated by small-scale dynamo; (3), high-energy scattering, where particles are only weakly scattered.

from the larger scale field will be smaller (if  $l_2 > r_{g1}$ , then the deflection angle  $e\delta B(l_2)r_{g1}/E < 1$ ); (c) – the deflection from some smaller scale  $l_1$  is also smaller (it is a random walk with  $r_{g1}/l_1$  steps), and the deflection angle is  $e\delta B(l_1)l_1^{1/2}r_{g1}^{1/2}/E < 1$ <sup>16</sup>). Assuming  $E = pc$  from here on, the  $D_{xx}$  and  $D_{pp}$  for such particles will be determined by velocity perturbations on scale  $r_{g1}$ , i.e.,  $u_s r_{g1}^{1/3} L^{-1/3}$ ; thus,

$$D_{xx} = (E/e\delta B^*)^{4/3} (L^*)^{-1/3} c, \quad (11)$$

$$D_{pp} = p^2 u_s^2 r_{g1}^{-1/3} L^{-2/3} / c \propto E^{14/9} \quad (12)$$

Finally, for very high energy particles, such as

$$E \gg e\delta B^* L^{\frac{1-\alpha}{2}} (L^*)^{\frac{1+\alpha}{2}} = e\delta B^* L^{3/4} (L^*)^{1/4}, \quad (13)$$

the trajectory will be a random walk with small deflections from scale  $L$  and an effective mean free path of  $E^2/e^2\delta B_L^2 L$ . The  $D_{pp}$  will be energy independent, as it will be set by the outer scale velocity perturbations of  $u_s$ . Consequently,

$$D_{xx} = E^2 c / e^2 \delta B_L^2 L, \quad (14)$$

$$D_{pp} = (e\delta B_L)^2 L u_s^2 / c^3. \quad (15)$$

#### 4.2. Low energy particle scattering

The scattering of gyrating particles in a strong mean field has been studied for a long time (e.g., Jokipii, 1966), and an associated so-called quasi-linear theory (QLT) of scattering has been formulated. A particular property of MHD turbulence — its strong anisotropy — makes particle scattering from solenoidal modes (e.g., Alfvén) fairly inefficient (Chandran 2000, Yan & Lazarian 2002). So, the compressive fast mode, which is rather isotropic, has been proposed as a more efficient scatterer in such settings (Yan & Lazarian 2002, 2004). The fast mode, however, can be strongly damped in realistic ISM environments, which causes scattering through the fast mode to depend on the properties of the gas, such as temperature, density and ionization fraction. For the purpose of this paper we ignore complicated issues of low energy scattering and acceleration and provide two simple, contrasting cases.

First, we can assume that the fast mode is fully damped and that only solenoidal modes survive on scales of  $L^*$  and smaller. In this case we can neglect QLT contributions from the Alfvénic and slow modes as they are very small. On the other hand, there are strong perturbations of the magnetic field on the outer scale of  $L^*$ . In this case particles, regardless of energy (provided that  $E \ll e\delta B(L^*)L^*$ ) are going to be reflected by magnetic bottles on scale  $L^*$  and  $D_{xx}$  will be independent of energy and equal to  $L^*c$ , while  $D_{pp}$  will be determined by the speed of the bottles. Thus,

$$D_{xx} = L^*c, \quad (16)$$

$$D_{pp} = p^2 u_s^2 (L^*)^{-1/3} L^{-2/3} / c. \quad (17)$$

Similar expressions can be derived from TTD resonance in the presence of large magnetic field perturbations (Yan & Lazarian 2008). Both of these diffusion rates smoothly transition to the solutions from previous section.

Alternatively, we can assume that the fast mode is not damped and that the scattering and second-order acceleration are due to the fast mode. If we assume that the amplitude of the fast mode is approximately in equipartition with other modes on the outer scale of sub-Alfvénic turbulence,  $L^*$ , we will obtain expressions that also smoothly transition to higher energy expressions from the previous section; namely,

$$D_{xx} = c r_{g2}^{1/2} (L^*)^{1/2}, \quad (18)$$

$$D_{pp} = p^2 u_s^2 (L^*)^{1/6} L^{-2/3} r_{g2}^{-1/2}, \quad (19)$$

(see, e.g. Yan & Lazarian 2004). Here we have used so-called acoustic turbulence scaling  $\delta B \sim l^{1/4}$  for the isotropic fast mode, as in Cho & Lazarian (2002).

It is also possible that in the shock acceleration regions, where the density of CRs is high, the scattering is affected by collective effects where compressions of magnetic field induce the gyroresonance instability in the fluid of compressed CRs as discussed in Lazarian & Beresnyak (2006). We do not provide a discussion of this more complex case here.

<sup>16</sup> Provided that the spectrum is falling ( $\alpha < 0$ )

Turbulent heating provided by solenoidal motions will be of the order of the turbulent rate,  $\epsilon = \rho v_s^3/L$ . However, this assumes that the turbulent cascade dissipates all of its energy into thermal particles. This might not be true for efficient second-order acceleration of low-energy particles. In particular, if the spectrum of CRs is sufficiently soft (steep), the second order acceleration will drain energy from turbulence and put it into CRs as particles would tend to diffuse to higher energies. On the other hand, if the spectrum is sufficiently hard (shallow), energy carried by high energy CRs may be able to drive turbulence<sup>17</sup>. In principle, one would like to monitor energy obtained or lost by CRs due to second-order acceleration/deceleration and adjust turbulent heating rates accordingly.

As a second note we mention that it is reasonable to believe that dissipation from secondary shocks (similar to ISM turbulent slow shocks) created in the precursor is going to be comparable to  $\epsilon$ . The above considerations leave a certain degree of uncertainty in the amount of thermal heating in our model.

## 6. DISCUSSION

### 6.1. Evolution of the ideas on shock acceleration

The problem of nonlinear diffusive shock acceleration (DSA) is a mature area of research with many publications since the original linear theory papers of Krymsky (1977), Bell (1978), Axford et al (1977) and Blandford & Ostriker (1978). Most of this research was motivated by the observed CR power-law distribution, and the apparent robustness of the basic model. The emphasis was largely, but not exclusively, on the predicted properties of CRs, rather than the physical details of their scattering. So as long as the acceleration process was described by rather simple and well-grounded convection-diffusion equation (1), the details of scattering and fluid dynamics have only had to be “reasonable” in order to obtain applicable results. On the other hand, since many reasonable models of the detailed scattering physics were proposed, there were, in effect, many models of DSA. One of the popular models to account for the scattering is based on a linear ( $\delta B < B$ ) or “almost linear” ( $\delta B \sim B$ ) streaming instability analysis. The most common application of the latter case is so-called Bohm scattering (m.f.p.  $\sim$  Larmor radius). While these models result in internally consistent particle spectra as well as the one-dimensional structure of the flow (see, e.g., Malkov 1998; Berezhko & Ellison 1999; Blasi 2002; Kang & Jones 2007), the question of physical justification remains.

Another approach has been to elicit some robust properties of the acceleration process without regard to underlying particle-fluid interactions (see a review of Malkov & Drury 2001 and references therein), although these studies emphasized the uncertainties in such important quantities as the predicted high energy cutoff of accelerated protons. This understanding is critical to a resolution of the origins of galactic cosmic rays, and especially the so-called “knee”. Furthermore, the higher energy frontier is more generally important in astrophysics, as it could set limits to physics of what is happening in

such objects as AGNs or core-collapsed supernovae. Indeed, while low-energy CRs can be accelerated in almost any source, the highest energy CRs require a combination of large magnetic field and large correlation length  $B_l l$  to be contained in the source. Otherwise, they easily escape. Present day neutrino experiments, such as ICE-CUBE, have set an ambitious goal to peek into the hearts of these objects, and obtain high-energy CR properties free of uncertainties associated with models of escape and propagation.

Recently, the DSA problem has been reconsidered again with regard to the problem of acceleration with more realistic scattering (Malkov & Diamond 2006) and the fluid dynamics in the presence of both the strong streaming instability and strong compressibility (Diamond & Malkov 2007). The latter approach uses the advection-diffusion equation with one spatial and one spectral dimension and assumes weak wave coupling. This is unlikely to be enough to describe three-dimensional compressive MHD turbulence (see the discussion in §1). Also, we point out that a classic streaming instability with a prescribed direction of the CR gradient along magnetic field is unlikely to be useful in a turbulent, strongly amplified field. Although our model is at this point phenomenological in its treatment of strongly compressible turbulence and uses this compressibility to estimate solenoidal motions that generate magnetic fields, we believe that we provided a more realistic description of the magnetic fields generation in the preshocked gas.

Generation of the magnetic fields in the postshock region was considered in many publications with both numerical and phenomenological means (see, e.g., Cowsik & Sarkar 1980, Giacalone & Jokipii 2007, Sironi & Goodman 2007, Inoue et al, 2009). Sironi & Goodman (2007) estimated a vortical energy that appears after GRB afterglow shocks due to preexisting density inhomogeneities. However it assumed that the magnetic field reaches equipartition with vortical energy and did not discuss the structure of the magnetic field. We argue that it is the shock precursor fields which are important. Also, the spectrum and the structure of this field are paramount for understanding physically motivated scattering coefficients. Inoue et al (2009) provided a detailed two-dimensional numerical study of post-shock turbulence and dynamo action. Two-dimensional dynamics, however is very different from a three-dimensional one (see, e.g., Biskamp 2003).

### 6.2. Current limitations of the numerical approach

The full numerical treatment of the highly-compressible flows in question is difficult. One-dimensional studies of such flows are meaningless, as they are likely to produce a picture which is completely different from three-dimensional dynamics. Indeed, one-dimensional flows necessarily generate shocks in a finite time, and the dynamics are fully dominated by those shocks (see, e.g. Suzuki et al 2007). The three-dimensional dynamics is more complicated, with compressible motions containing only a fraction of energy and weak sub-shocks playing some, but not necessarily a dominant role. Direct three-dimensional simulations of supersonic turbulence are not only computationally expensive, but inherently limited in

<sup>17</sup> This process is qualitatively depicted in § 2. The precursor can generate velocity fluctuations due to inhomogeneity of the precursor pressure by a variety of mechanisms.

a number of ways. The best known limitation is the range of scales (typically a useful range of scales in a fairly computationally expensive  $1024^3$  simulation is 4-200 in grid units). More relevant to the DSA problem, however, is the limitation in sonic Mach number, which is around 20 for a  $1024^3$  simulation and is determined by having strongly compressible motions ( $v \sim c_s$ ) on the grid cell scale, or having a significant fraction of matter accumulated in clumps of the grid cell size. The requirement of the DSA problem, however, is not  $M_s \sim 20$  but rather can be  $M_s \sim 1000$  or even higher in more energetic sources (AGNs, relativistic jets in GRB sources). In this situation three-dimensional fluid-PIC codes that will aim to describe interacting fluid and CRs will suffer from the same limitations as fluid codes, but also will be unable to describe a huge spread in energies of the CR spectrum, due to limited statistics of particles.

### 6.3. The source of solenoidal motions

In §2 we assumed that the solenoidal velocity is a fraction of the velocity drop along the precursor with the main mechanism being the pre-existing density inhomogeneities and the precursor pressure field. We noted that we expect this mechanism to be fairly efficient (i.e.  $A_s$  close to unity) as long as preexisting density perturbations  $\delta\rho/\rho$  are of the order unity. However, it is interesting to consider the possibility that the initial density perturbations are enhanced *by the precursor* to this level. For instance, once the total pressure in the precursor,  $P$ , is dominated by CRs, the weak coupling between fluid fluctuations and CRs leads to regions in the precursor where  $\nabla P \cdot \nabla \rho < 0$ . This is unstable to Rayleigh-Taylor-like instabilities that have been shown to strongly enhance turbulence in CR modified shocks (Ryu et al. 1993). While these effects have been demonstrated, the resulting solenoidal turbulence has not yet been quantitatively evaluated. Therefore, we cannot conclude that  $A_s$  could be considered a small parameter even if the inflowing density perturbations are small.

Aside from inflowing density inhomogeneities, another possible mechanism of generating turbulence is related to the inhomogeneities in the precursor CR density, or, more generally, a dynamic three-dimensional turbulent interaction between fluid and CR's, which allows exchange of energy in both directions. This includes instabilities discussed above. Qualitatively, this effect also works to create additional solenoidal motions. However, this is a more complicated phenomenon that will be studied elsewhere.

We expect the current instability, which is considered in detail in the next subsection, to generate density and solenoidal velocity perturbations as well. However, due to the limitations of the numerical approach (see the previous subsection) the dynamics of density in the nonlinear stage of current instability is not fully understood.

### 6.4. Our approach and current driven instability

In response to the realization that magnetic fields could be amplified significantly compared to the background field, a model based on a current-driven instability was proposed and tested numerically (Bell 2004, Vladimirov et al. 2006; Zirakashvili et al 2008, Riquelme

& Spitkovsky 2009). In the linear instability stage the magnetic field grows fastest on the characteristic scale, determined by the initial field  $B_0$ , and the current  $j_d$ ,

$$l = 1/k_c = \frac{cB_0}{4\pi j_d}, \quad (20)$$

where  $j_d$  is from high-energy CRs that are “rigid” enough to have  $qB_0/pc \ll k_c$  (Bell 2004). The linear growth rate depends only on the current according to the relation

$$\gamma = \frac{j_d}{c\sqrt{\frac{\rho_0}{\pi}}}. \quad (21)$$

The nonlinear saturation stage is characterized by slower growth on larger scales (Bell 2004, Zirakashvili et al 2008). This growth, however, advects along with the fluid and, as we discussed in § 2, has to be limited by the time for flow to cross the precursor. It is also worth noting that Bell (2004) and Zirakashvili et al (2008) used weakly compressible simulations with initial conditions that did not have strong perturbations in either fluid density or CR density, which makes it totally different from our approach. We believe, there is a good physical reason why precursor turbulence is often strongly compressible and inhomogeneous (see §2).

One can compare growth rates of magnetic energy, provided by the small-scale dynamo (eq. 8) and current-driven instability (eq. 21), assuming that the current-driven instability is in the stage with  $\delta B \sim B_0$ , but the linear growth rate still holds. The result is

$$\frac{dB_{cur}^2}{dB_{dyn}^2} = 52 \cdot \frac{j_d L}{cB_0} \cdot \left(\frac{v_{A0}}{u_s}\right)^3. \quad (22)$$

The second part of the RHS in eq. (22) can be estimated from the characteristic  $v_A$  of the ISM ( $\sim 10\text{km/s}$ ) and could be as small as  $10^{-9}$ , if the shock speed is large ( $\sim 10000\text{km/s}$ ). The first part of the RHS of eq. (22) can be interpreted as the ratio of the field created directly by the high-energy particle current on scale  $L$  to the initial field  $B_0$ . The robust estimate of the current  $j_d$ , however, seems pretty elusive. Suppose, following Riquelme & Spitkovsky (2009), we assume that the current is produced entirely by escaping particles and that there is a fixed ratio  $\eta_{esc} \approx 0.05$  between the flux of CR energy emitted by the shock and the flux of energy of the incoming fluid  $\rho u_{sh}^3/2$  and also assume that a characteristic energy of escaping particles is  $E_{esc} = 10^{15}$  eV. Then one can numerically estimate the above ratio. Taking  $L = 1\text{pc}$  and assuming  $u_s \approx 0.5u_{sh}$  (since we assume that the shock is strongly modified, i.e.  $u_{sh} = u_0 \sim u_0 - u_1$  and  $A_s$  is of the order unity), we get

$$\begin{aligned} \frac{dB_{cur}^2}{dB_{dyn}^2} &= 1.6 \times 10^{-4} \left(\frac{10^{15}\text{eV}}{E_{esc}}\right) \left(\frac{\eta_{esc}}{0.05}\right) \left(\frac{L}{1\text{pc}}\right) \\ &\times \left(\frac{B_0}{5\mu\text{G}}\right) \left(\frac{v_{A0}}{12\text{km/s}}\right) \left(\frac{0.5u_{sh}}{A_s(u_0 - u_1)}\right)^3. \end{aligned} \quad (23)$$

This difference in field growths is due to the fact that in our model the full pressure ( $\sim$  energy density) of the CRs is behind the force that winds up magnetic fields, while the driving force of the current instability model



comes only from those CRs that are able to freely stream a substantial distance through the flow. The efficiency of our model is based on an assumed large value of  $A_s$  parameter (of the order unity). Also we do not consider the feedback of CRs to the full three-dimensional fluid dynamics, assuming instead that CR pressure is homogeneous in two directions along the shock.

### 6.5. Future work

The self-consistent treatment of the flow profile and acceleration of particles using expressions from § 4 will be presented in a future publication. The scattering coefficients assume that efficient scattering and acceleration will be provided for particles with energies up to  $E_{2-3} = e\delta B^* L^{*1/4} L^{3/4}$  (see Fig. 4). This energy can be estimated taking  $u_s \tau \approx L$ ,  $u_s \approx 10^4 \text{ km/s}$  and  $L \approx 1 \text{ pc}$  as  $E_{2-3} \approx 3 \times 10^{17} \text{ eV}$ . This energy corresponds to a mean free path of the order of  $L$ . However, as the acceleration efficiency is smaller by a factor of  $u_s/c$  (Hillas, 1984) the maximum acceleration energy will be around  $10^{16} \text{ eV}$ . The higher energy particles will be scattered relatively less efficiently and likely to form a steeper spectrum. This estimate is tentative and needs to be confirmed or corrected as the self-consistent treatment of Eq. (1) and the evolving structure of the precursor and will be available from the future work.

Finally, we would like to mention that field growth in our model could be amended by the consistent description of the front-running region of the precursor where turbulence is not yet developed. At this point, however, it is not clear whether this region will be dominated by the classic streaming instability, strong compressible effects (and, possibly, generation of secondary fast shocks, as the magnetic field is not yet amplified to prevent creation of those), or the current-driven instability.

## 7. SUMMARY

In order to explain efficient acceleration of high-energy CRs in supernova shocks we appealed to magnetic field amplification in the shock precursor that is induced by the small scale turbulent dynamo. In our picture the velocity field necessary for such amplification appears hydrodynamically as a result of the strong CR pressure gradient acting on an initially *inhomogeneous* medium in the preshock region. We assumed efficient conversion of the precursor velocity drop into solenoidal motions due to strong density perturbations of the inflowing fluid. We also ignored CR inhomogeneities appearing as a back-reaction and their nonlinear feedback. We estimate that magnetic fields produced by such amplification are able to efficiently scatter and accelerate CRs with energies up to  $10^{16} \text{ eV}$ .

We are grateful to Misha Malkov, Pat Diamond, Anatoly Spitkovsky and Brian Reville for fruitful discussions. We are grateful to the anonymous referee for helpful, meticulous comments. AB thanks the IceCube project for support of his research. TWJ acknowledges support from NASA grants NNG05GF57G and NNX09AH78G, as well as the Minnesota Supercomputing Institute. AL acknowledges the NSF grants ATM 0648699, AST 0808118 and the NASA grant NNX09AH78G.

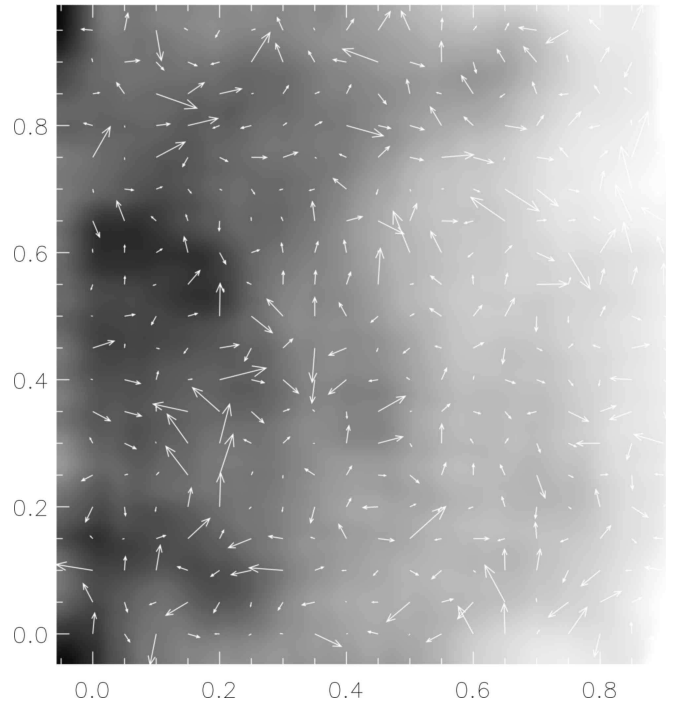


FIG. 5.— A 2D slice of the 3D particle tracing experiment, showing magnetic field projection on the plane (arrows) and particle density using grayscale (dark being higher density).

## 8. APPENDIX A

In order to demonstrate that the stochastic field generated in the cosmic ray precursor will be hard to treat properly in the classic streaming instability approach, we ran particle tracing simulations in a stochastic three-dimensional field, generated by a small scale dynamo (discussed in §3).

The electromagnetic field was obtained through direct three-dimensional numerical simulation of the incompressible MHD equations with turbulent driving, along with a zero mean field and small fluctuations as initial conditions. The simulation was similar to MHD2b0h, described in Beresnyak & Lazarian (2009b), with the exception that it was run for a relatively short time while the small-scale dynamo was in its linear stage (see §3). The time was chosen so that the equipartition scale  $L^*$  was approximately in the middle of the logarithmic range of scales. The electric field was obtained assuming  $v_A/c = 10^{-5}$ .

The particles were injected on one side of the cube and their relativistic equation of motion was solved by a hybrid quality-controlling Runge-Kutta ODE solver. The particles were injected from the left and escaped to the right. Fig. 5 presents a slice of this three-dimensional experiment, where magnetic fields are represented by arrows and the CR particle density by grayscale. We see, that aside from the obvious left-to-right global gradient we cannot identify any clear structure of particle density along the field. This invalidates in this case the assumption of the classic streaming instability, which requires a regular particle density gradient along the field lines to produce a regular field-aligned number density current.

## REFERENCES

- Armstrong, J. W., Rickett, B. J., & Spangler, S. R. 1995, ApJ, 443, 209
- Axford, W. I., Leer, E., & Skadron, G. 1977, ICRC, 11, 132
- Bell, A. R. 1978, MNRAS, 182, 147
- Bell, A. R. 2004, MNRAS, 353, 550
- Beresnyak, A., Lazarian, A. & Cho 2005, ApJ, 624, L93
- Beresnyak, A., Lazarian, A. 2008, ApJ, 678, 961
- Beresnyak, A., Lazarian, A. 2009a, ApJ, 702, 460
- Beresnyak, A., Lazarian, A. 2009b, ApJ, 702, 1190
- Berezhko, E. G. & Ellison, D. C. 1999, ApJ, 526, 385
- Biskamp, D. 2003, *Magnetohydrodynamic Turbulence*. (Cambridge: CUP)
- Blandford, R. D., Ostriker, J. P. 1978, ApJ, 221, 29L
- Blasi, P. 2002, APh, 16, 429
- Blasi P. & Amato, E. 2008, 2008ICRC, 2, 235
- Chandran B.D.G. 2000, Phys. Rev. Lett., 85, 4656
- Chandran B.D.G. 2005, Phys. Rev. Lett., 95, 26, 265004
- Cho, J. & Lazarian, A. 2002, Phys. Rev. Lett., 88, 5001
- Cho, J. & Vishniac, E. 2000, ApJ, 539, 273
- Cho, J., Vishniac, E., Beresnyak, A., Lazarian, A., & Ryu, D. 2009, ApJ, 693, 1449
- Cowsik, R., Sarkar, S., 1980, MNRAS, 191, 855
- Diamond, P.H., Malkov, M.A. 2007 ApJ, 654, 252
- Dorfi, E. A. & Drury, L. O'C. 1985, Proc. 19th I.C.R.C. (La Jolla) 3, 121
- Drury, L.O'C. 1984, Adv. Space Res., 4, 185
- Elmegreen, B. G., Scalo, J. 2004, ARA&A, 42, 211
- Galtier, S., Nazarenko, S.V., Newel, A.C., Pouquet, A., J. Plasma Phys. 2000, 63, 447
- Ginzburg, V. & Syrovatskii, S. 1964, Origin of Cosmic Rays, Pergamon Press, NY
- Goldreich, P. & Sridhar, S. 1995, ApJ, 438, 763
- Giacalone J., Jokipii, J.R. 2007, ApJ, 663, L41
- Heiles, C. 1997, ApJ, 481, 193
- Hillas, A. M. 1984 ARA&A, 22, 425
- Inoue, Yamazaki, & Inutsuka 2009, ApJ, 695, 825
- Jokipii, J. R. 1966, ApJ, 146, 480
- Kang, H., Jones, T. W., & Ryu, D. 1992, ApJ, 385, 193
- Kang, H., Jones, T.W. 2007, Astropart. Phys. 28, 232
- Kang, H., Ryu, D. & Jones, T. W. 2009, ApJ, 695, 1273
- Kazantsev A.P. 1967, Sov. Phys. JETP, 26:1031 (1968)
- Krymsky, G.F. 1977, Sov. Phys. Dokl. 23, 327
- Kulsrud R.M., Anderson S.W. 1992, ApJ, 396, 606
- Lagage, P. O. & Cesarsky, C. J. 1983, A.&A. 125, 249L
- Lazarian, A., Beresnyak, A. 2006, MNRAS, 373, 1195
- Lazarian, A., Opher, M. 2009, ApJ, in press
- Lucek, S.G., Bell, A.R. 2000, MNRAS, 314, 65
- Malkov, M.A., Diamond, P.H. 2006, ApJ, 642, 244
- Malkov, M. A. 1998, Phys. Rev. E., 58, 4911
- Malkov, M.A., Drury, L.O'C. 2001, Rep. Prog. Phys. 64, 429
- Maron, J., & Goldreich, P. 2001, ApJ, 554, 1175
- McKee, C. & Ostriker, E. 2007, ARA&A, 45, 565
- Riquelme, M. A. & Spitkovsky, A. 2009, ApJ, 694, 626
- Ryu, D., Kang, H. & Jones, T. W. 1993, ApJ, 405, 199
- Schekochihin, A. & Cowley, S. 2007, in *Magnetohydrodynamics - Historical evolution and trends*, eds. by S. Molokov, R. Moreau, & H. Moffatt (Berlin; Springer), p. 85. (astro-ph/0507686)
- Sironi, L., Goodman, J. 2007, ApJ, 671, 1858
- Skilling, J. 1975, MNRAS, 172, 557
- Suzuki, T. K., Lazarian, A., Beresnyak, A., 2007, ApJ, 662, 1033
- Vishniac, E. T., Cho, J. 2001, ApJ, 550, 752
- Vladimirov, A., Ellison, D. C. & Bykov, A. 2006, ApJ, 652, 1246
- Völk, H.J., Drury, L.O'C., & McKenzie, J.F. 1984, A&A, 130, 19
- Yan, H. & Lazarian, A. 2002, Phys. Rev. Lett., 89, 1102
- Yan, H. & Lazarian, A., 2004, ApJ, 614, 757
- Yan, H. & Lazarian, A., 2008, ApJ, 677, 1401
- Zeldovich Ya.B., Ruzmaikin A.A., Molchanov S.A., & Sokoloff D.D. 1984, J Fluid Mech, 144, 1
- Zirakashvili, V. N., Ptuskin, V. S., & Volk, H. J. 2008, ApJ, 678, 255